2016

Extremely low material loss and dispersion flattened TOPAS based circular porous fiber for long distance terahertz wave transmission

Islam, Saiful

Elsevier

http://dx.doi.org/10.1016/j.yofte.2016.11.014

Extremely Low Material Loss and Dispersion Flattened Topas Based Circular Porous Fiber for Long Distance Terahertz Wave Transmission

Article *in* Optical Fiber Technology · January 2017

DOI: 10.1016/j.yofte.2016.11.014

Md. Saiful Islam
University of Adelaide

Jakeya Sultana
University of Adelaide

Sohel Rana
Boise State University

Mohammad Rakibul Islam
Islamic University of Technology

Optical Fiber Technology 34 (2017) 6–11

Contents lists available at ScienceDirect

Optical Fiber Technology

www.elsevier.com/locate/yofte

Regular Articles

Extremely low material loss and dispersion flattened TOPAS based circular porous fiber for long distance terahertz wave transmission

Md. Saiful Islam [a,*], Jakeya Sultana [a], Sohel Rana [b], Mohammad Rakibul Islam [a], Mohammad Faisal [c], Shubi F. Kaijage [d], Derek Abbott [e]

[a] Department of Electrical and Electronic Engineering, Islamic University of Technology, Gazipur 1704, Bangladesh
[b] Department of Electrical and Electronic Engineering, Rajshahi University of Engineering & Technology, Rajshahi 6204, Bangladesh
[c] Department of Electrical and Electronic Engineering, Bangladesh University of Engineering & Technology, Dhaka 1000, Bangladesh
[d] Department of Communication Science and Engineering, School of Computational and Communication Science and Engineering, Nelson Mandela African Institution of Science and Technology, Arusha 23311, Tanzania
[e] School of Electrical and Electronic Engineering, The University of Adelaide, SA 5005, Australia

ARTICLE INFO

Article history:
Received 12 July 2016
Revised 11 November 2016
Accepted 30 November 2016

Keywords:
Optical fiber
Terahertz
Effective material loss
Dispersion
Photonic crystal fiber

ABSTRACT

In this paper, we present a porous-core circular photonic crystal fiber (PC-CPCF) with ultra-low material loss for efficient terahertz wave transmission. The full vector finite element method with an ideally matched layer boundary condition is used to characterize the wave guiding properties of the proposed fiber. At an operating frequency of 1 THz, simulated results exhibit an extremely low effective material loss of 0.043 cm^{-1}, higher core power fraction of 47% and ultra-flattened dispersion variation of 0.09 ps/THz/cm. The effects of important design properties such as single mode operation, confinement loss and effective area of the fiber are investigated in the terahertz regime. Moreover, the proposed fiber can be fabricated using the capillary stacking or sol-gel technique and be useful for long distance transmission of terahertz waves.

1. Introduction

For the last few years, researchers have been concentrating their attention on the terahertz band for its numerous technological applications in the fields of sensing [1], biotechnology [2], imaging [3–5], spectroscopy [6] and communication [7] etc. At present, long distance transmission of terahertz waves is limited due to higher material absorption loss. Still now, most of the terahertz transmission depends on free space for its wave propagation [8]. Dependency on free space has some undesirable problems such as sensitive alignment, path loss, uncertain absorption loss and difficult integration with other components. To overcome these problems, various kinds of guided transmission media have been previously reported [9–13].

At the early stages of development of guided transmission media, researchers showed that metallic wires [9] and metal-coated dielectric tubes [10] can be used as a transmission medium but the dilemma of using metal waveguides was due to high bending loss, low coupling efficiency and unbalanced guidance in a complex atmosphere [11,12]. Later, plastic subwavelength fibers [13] came into existence for their comparatively lower losses. However, most of the field propagates outside the waveguide core, thus resulting in strong coupling to the environment. For improvement, Nagel et al. [14] reported a fiber with the addition of a subwavelength hole within a solid core, which increases the guided field in the air hole, hence reducing the absorption losses. However, the loss due to the material was still high.

A research breakthrough occurred when polymer materials were used instead of metals allowing a much lower absorption loss. The polymer materials PMMA [15], Teflon [16], TOPAS [17], Zeonex [18] etc can be used as the initial choices for THz waveguidance. However, PMMA and Teflon were not considered in the design of our waveguide because of their higher losses than TOPAS and Zeonex [19]. Note that, TOPAS was used as the bulk material in our designed PCF. The motivation behind using TOPAS rather than other materials includes, (i) lower material absorption loss, (ii) low density, (iii) glass transition temperature much higher than PMMA [20], (iv) multi-antibody biosensing [21], (v) high transparency, (vi) humidity insensitive [22], (vii) excellent biocompatibility, (viii) constant refractive index n = 1.53 in the frequency range of 0.1–1.5 THz [17], (ix) negligibly hygroscopic [23], which results in lower terahertz absorption and is advantageous for manufacturing terahertz waveguides. Zeonex on the other side is an ultra high

* Corresponding author.
E-mail address: saiful.ruet.ete@gmail.com (M.S. Islam).

http://dx.doi.org/10.1016/j.yofte.2016.11.014
1068-5200/

purity optical grade polymer widely used in optical applications where refractive index stability over a high temperature and humidity range is crucial. Please note that, TOPAS and Zeonex can be drawn together into a single mode step-index fiber [24].

To reduce the material absorption loss further, polystyrene foam [25] was introduced but it required much larger dimensions. Hollow core Bragg fibers [26–27] were also introduced but disregarded due to their unwanted narrow band properties. Photonic crystal fiber (PCF) [17] is a micro-structured optical waveguide with finite number of air holes in the cladding. Note that a PCF with solid cores has been introduced but it is found that the material absorption loss of solid core is too high [17] and almost equal to the bulk absorption loss of the used material. Recently, to improve field confinement and reduce effective material loss (EML) further, studies have used a porous core surrounded by air cladding [29].

To date researchers have proposed several polymer waveguides, of which porous core PCF's [29–35] gained much attention. The distinction between porous core PCF and conventional PCF is that the solid core of the conventional PCF is replaced by number of smaller air holes in the porous core PCF. Based on the concept of porous core, both porous core and hollow core honeycomb bandgap fiber have been proposed [36] and after numerical and experimental investigation, studies have found that porous core fiber has wider bandgap, lower total propagation loss and is easier to manufacture than hollow core fiber.

For characterization of terahertz porous fibers Atakaramians et al. [28] developed a technique by exploiting a micro-machined photoconductive probe-tip. They showed a loss less than 0.08 cm^{-1} within the frequency range of 0.2–0.3 THz with minimal loss of 0.03 cm^{-1} at a frequency of 0.24 THz. Mechanically down-doped low loss directional couplers were also proposed [43,44] for broadband terahertz applications. The down-doping was achieved by introducing micro-structured air holes in the core.

In 2013, Kaijage et al. [29] proposed a porous core octagonal photonic crystal fiber with TOPAS as the base material for terahertz wave guidance. They realized an effective material loss of 0.076 cm^{-1} but did not perform analysis for dispersion and core power fraction properties of the fiber. Later, Raonaqul et al. [30] reported a porous core fiber having a rotated hexagonal core structure and a hexagonal cladding structure. Later Rana et al. [31] proposed a porous fiber having octagonal structure in both core and cladding. They were able to reduce the EML further to 0.058 cm^{-1} although omitted to characterize the dispersion properties. However, Hasan et al. [32] proposed a fiber having a circular structure in the core and an octagonal structure in the cladding. They demonstrated a comparatively lower EML of 0.056 cm^{-1} without exploring the single-mode limits of the fiber. Furthermore, Raonaqul et al. [33] proposed a circular structure in both core and cladding. They showed comparatively lower EML of 0.053 cm^{-1} with dispersion flattened properties. In 2015, H. Bao et al. [19] proposed a dielectric tube waveguide with absorptive cladding for broadband applications. Raonaqul et al. [34] proposed a low-loss diamond core porous fiber having EML of 0.07 cm^{-1}, but the loss is actually higher. Later, Hasan et al. [35] proposed a slotted core kagome lattice terahertz fiber and showed an EML of 0.05 cm^{-1}, however the problem is that the loss is still higher and the fabrication of slotted core is difficult. Recently, Saiful et al. [37] proposed another waveguide with octagonal structure in the cladding and a rotated hexagonal structure in the core. They showed comparatively lower EML and flatten dispersion profile when 49.1% useful light propagates through the core.

For further improvement, a TOPAS based porous fiber having hexagonal array of air-holes in the core and circular array of air-holes in the cladding structure is presented in this paper. The EML of the proposed fiber is 0.043 cm^{-1}, which is about 78.5% less than the bulk absorption material loss of TOPAS and almost half of the useful power goes through the core air holes. As the propagation of light through our designed fiber is based on modified total internal reflection (MTIR), the effects of external environment can totally be neglected. Thus it is expected that the fiber can efficiently be applied to the transmission of broadband terahertz waves.

2. Model design

Fig. 1 depicts the proposed fiber with an enlarged version of the core. In the designed PC-CPCF, five rings of air holes for circular cladding and three rings of air holes for hexagonal core structure are considered.

The spacing between two adjacent air holes in the cladding on two adjacent rings is denoted by Λ. The spacing between air holes lying on the same ring is Λ_1, which is related to Λ by $\Lambda_1 = 0.765\Lambda$. For the core, the spacing between two air-holes on two adjacent rings and that on the same ring is Λ_c. The diameter of air holes in cladding region is denoted by d and $d1$. Two air holes in the first ring of the cladding are kept smaller than the other air holes with diameter $d1$. The presence of these smaller air holes in the first ring of the cladding made it possible to increase the core porosity that hence reduces the EML. Note that simulating this type of structure of the fiber does not introduce computational complexity. During simulation, with the variation of core diameter $D_{core} = 2(\Lambda - d/2)$, the air holes of diameter d were varied automatically but the air holes of diameter $d1$ were varied manually. The air filling fraction (AFF) d/Λ was kept fixed at 0.76 throughout the numerical analysis for a good confinement factor. The value of AFF should not be increased further due to fabrication difficulties. In the meantime, the AFF in the core diameter is intentionally varied and mostly determined by the core porosity. Porosity is defined as the ratio of the air hole area to the total cross-section area of the core.

3. Simulation procedure and results

The full vector finite element method (FEM) based software COMSOL, version 4.3b is used for simulating the characteristics of the fiber. A perfectly matched layer (PML) boundary condition is used to absorb the incident radiation without producing reflections, which is about 10% of the total fiber radius. The finalized geometry has 159 domains, 636 boundaries, and 636 vertices. The full structure contains 31,980 elements and 4515 boundary elements. The power flow distribution of the proposed fiber at different core porosities is shown in Fig. 2. It is observed from Fig. 2 that light is well confined inside the core of the fiber.

First, we have to be ensuring that the single mode condition of the proposed fiber is not affected with the modification of core diameter and frequency. Considering this fact, the single mode properties were analysed carefully by a parameter called V–parameter. Normalized frequency or V–parameter can be calculated by [27],

$$V = \frac{2\pi rf}{c}\sqrt{n_{co}^2 - n_{cl}^2} \leqslant 2.405, \quad (1)$$

where r is defined as the core radius, c is the speed of light in vacuum, n_{co} and n_{cl} are considered to be the refractive indices of core and cladding respectively. The core refractive index n_{co} is considered to be effective refractive index (n_{eff}) because of the porous core. Theoretically, we can assume n_{cl} to be unity because of the large number of air holes in the cladding [29–35], but practically it must be slightly greater than unity as cladding is a combination of air and material. The characteristics of the V–parameter are calculated for different values of n_{cl}. Thus, satisfying Eq. (1), it is observed from Figs. 3 and 4 that, as the n_{cl} increases with core

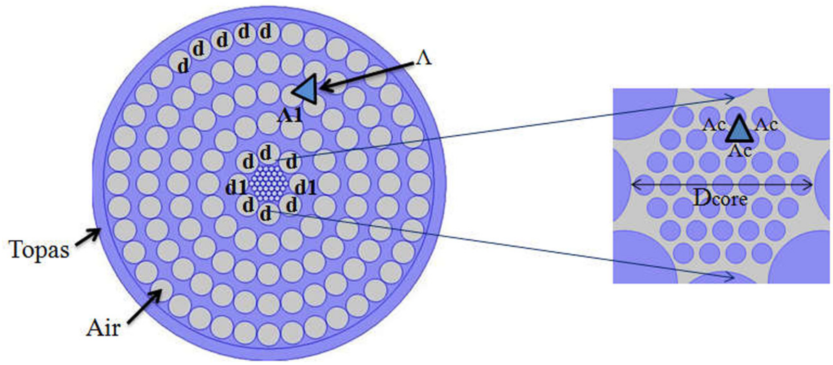

Fig. 1. Cross section of the proposed fiber with an enlarged view of its core.

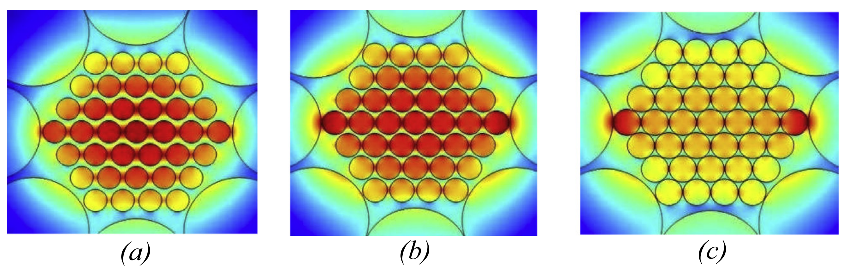

Fig. 2. Power flow distribution of the proposed PCF for (a) 61% (b) 71% (c) 81% porosity.

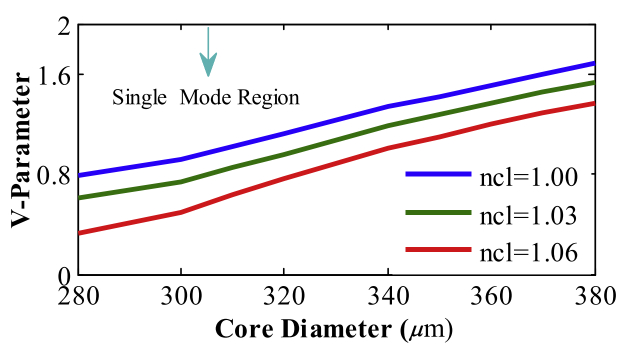

Fig. 3. V parameter versus core diameter with f = 1 THz and porosity = 81%.

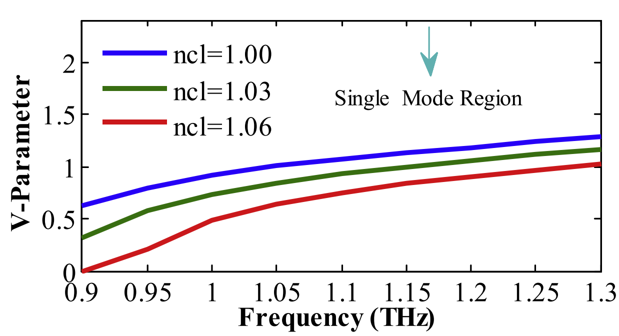

Fig. 4. V parameter versus frequency at D_{core} = 300 μm and porosity = 81%.

diameter and frequency, respectively, the range of single mode of the fiber is also increased.

Then we focus on absorption loss or effective material loss of the proposed fiber. The EML of a fiber can be calculated by [27],

$$\alpha_{eff} = \sqrt{\frac{\varepsilon_0}{\mu_0}}\left(\frac{\int_{mat} n_{mat}|E|^2\alpha_{mat}dA}{|\int_{all} S_z dA|}\right) \quad (2)$$

where ε_0 and μ_0 are considered to be the relative permittivity and permeability in vacuum respectively, n_{mat} is the refractive index of TOPAS, α_{mat} is the bulk material absorption loss, **E** is the modal electric field and S_z is the z component of the pointing vector $S_z = -½(\mathbf{E} \times \mathbf{H}^*)\cdot z$, where **E** and **H** are the electric and magnetic fields respectively. Fig. 5 depicts the characteristics of EML as a function of core diameter with different core porosities. It is clearly observable that, for the same porosity values EML is almost constant when the core diameter changes. The EML basically depends upon the amount of material used in the core. It is also observed from Fig. 5 that as the porosity decreases the EML increases. As the porosity decreases, the size of air holes in the core decreases which in turn increases the amount of material and thus increase EML. It is clearly depicted that at a core diameter of 300 μm and frequency of 1 THz, minimal EML of 0.043 cm^{-1} is obtained which is less than the previously proposed in Refs. [29–35].

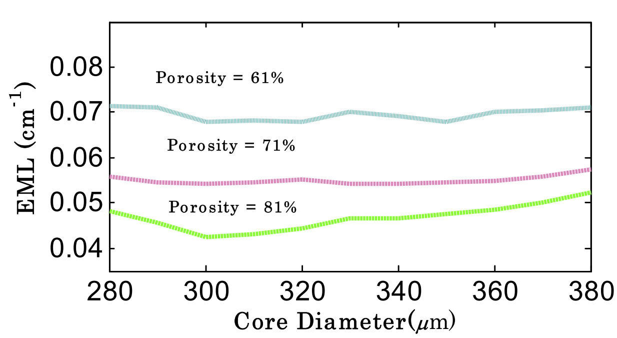

Fig. 5. Effective material loss as a function of core diameter at different porosities with f = 1 THz.

The amount of useful power propagating through the fiber core can be calculated by [38],

$$\eta' = \frac{\int_X S_z dA}{\int_{\text{all}} S_z dA} \quad (3)$$

where η' represents mode power fraction and X represents the area of interest. To design a standard PCF, it is necessary to pass most of the useful power through the core air holes. Higher D_{core} increases the core power fraction but with the increase of EML, on the contrary EML decreases with the decrease of D_{core} but this also decrease the core power fraction. These are contradictory conditions and need to select an optimum condition for getting higher core power fraction and lower EML. At different core porosities, the characteristics of core power fraction as a function of core diameter is shown in Fig. 6, where it can be observed that the amount of core power increases with the increase of core diameter. It is further observed from the same figure that, at 81% core porosity, f = 1 THz frequency and D_{core} = 300 μm shows 47% of the total power propagating through the core air holes which is sufficient for terahertz wave guidance.

Now, it is important to note that, in TOPAS, the bulk material absorption loss is not constant over the frequency range of 0.65–1.3 THz rather it increases linearly with frequency [39]. So, according to the empirical formula [39]: α (ν) = ν^2 + 0.63ν–0.13 [dB/cm], it is experimentally demonstrated through Fig. 7 that the bulk material absorption loss depends on frequency. This matter is carefully observed when calculating the frequency response loss characteristics of the fiber. From Fig. 8 one can deduce that as the frequency increases from 1 THz, the EML increases and core power fraction decreases. The electromagnetic frequency is proportional to the EML and hence as the frequency increases the EML also increases. Furthermore, from Fig. 8, it is evident that the EML is minimum and core power fraction is higher at an operating frequency of f = 1 THz with 81% core porosities.

Another important parameter to be considered for PCF design is confinement loss. It depends upon the core porosity and the number of air holes used in cladding. It can be calculated by taking the imaginary part of the complex refractive index. The confinement loss can be calculated by [18],

$$LC = 8.686\left(\frac{2\pi f}{c}\right)\text{Im}(n_{\text{eff}})\ \text{dB/m} \quad (4)$$

where f is the frequency of the guiding light, c is speed of light in vacuum and Im(n_{eff}) yields the imaginary part of the refractive index. The confinement loss as a function of frequency is shown in Fig. 9. from where it is observed that as the frequency increases, the confinement loss scaled down. In our designed fiber, at f = 1 THz, D_{core} = 300 μm and 81% porosity, a confinement loss of the order of $10^{-2.5}$ cm^{-1} is obtained which is negligible compared to the calculated EML.

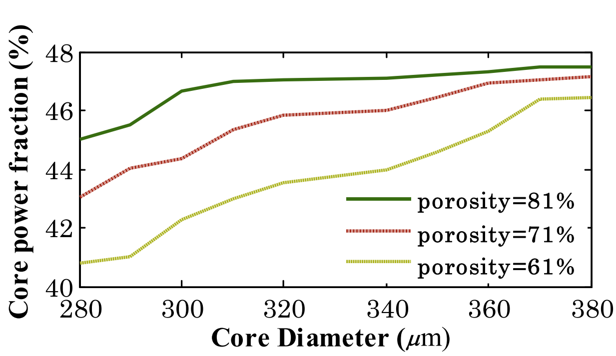

Fig. 6. Fraction of mode power through core air holes versus core diameter at different porosities at f = 1 THz.

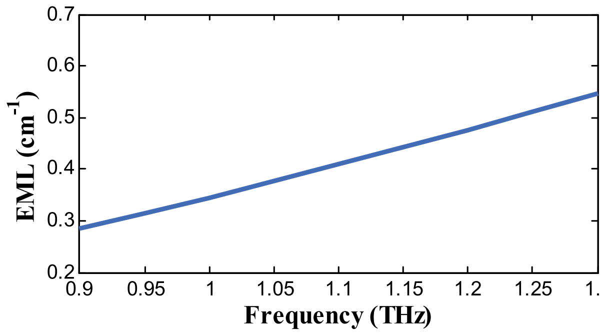

Fig. 7. Effective Material Loss vs frequency using empirical equation.

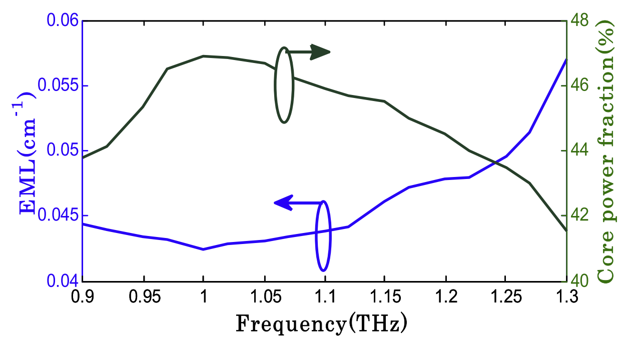

Fig. 8. Variation of EML with respect to frequency at D_{core} = 300 μm and porosity = 81%.

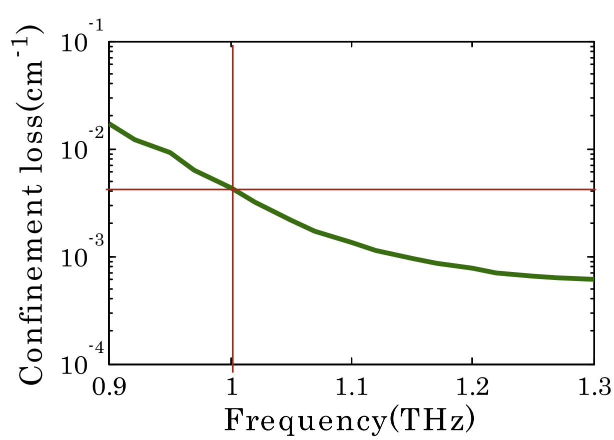

Fig. 9. Confinement loss as a function of frequency variation at D_{core} = 300 μm and porosity = 81%.

Next we discuss the dispersive properties of the proposed fiber. As stated in Ref. [39] that the refractive index of TOPAS is constant in between the frequency range of 0.1–1.5 THz, its material dispersion can totally be neglected in this band. So only the waveguide dispersion is analysed in our proposed fiber. The dispersion parameter (β_2) can be calculated by [18],

$$\beta_2 = \frac{2}{c}\frac{dn_{eff}}{d\omega} + \frac{\omega}{c}\frac{d^2 n_{eff}}{d\omega^2}. \quad (5)$$

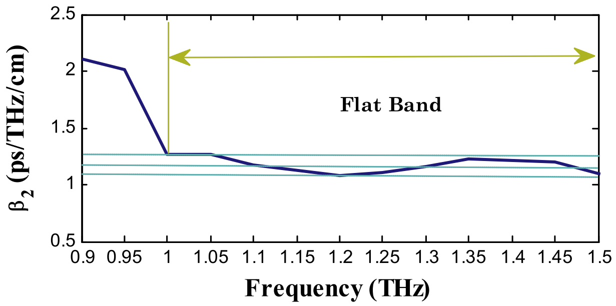

Fig. 10. Frequency dependent dispersion at D_{core} = 300 μm and porosity = 81%.

The calculated dispersion as a function of frequency is shown in Fig. 10. It can be observed from Fig. 10 that the flatness of dispersion is achieved from 1–1.3 THz where $\beta_2 < 1.23$ ps/THz/cm and $\beta_2 > 1.05$ ps/THz/cm, so the variation in dispersion is less than 0.09 ps/THz/cm.

The effective area (A_{eff}) of the proposed fiber is also addressed and can be calculated by [42],

$$A_{eff} = \frac{[\int I(r)rdr]^2}{[\int I^2(r)dr]^2} \quad (6)$$

where $I(r) = |E_t|^2$ is defined as the transverse electric field intensity distribution in the cross section of the fiber. The A_{eff} as a function of frequency is shown in Fig. 11, from where it is observed that as the frequency increases from 0.9 THz, the A_{eff} decreases. The reason being more light is confined in the core for $f > 1$ THz. It is also observed that at operating parameters, the calculated A_{eff} is very much comparable to those in Refs. [29,42].

Finally, it is necessary to discuss the fabrication possibilities for the fiber. Stack and drilling, capillary stacking and sol-gel techniques are the most commonly used techniques for PCF fabrication. As our proposed fiber comprised of circular air holes, capillary stacking [40] and sol-gel [41] techniques can be the best choice to fabricate our proposed PCF where the dimension of the designed PCF can be adjusted freely.

4. Conclusion

A comparatively simple single mode TOPAS based PC-CPCF with ultra-low material loss, higher core power fraction and ultra-flattened dispersion is proposed in this paper. The significance of our proposed PCF is extremely low EML and simplicity in design. Ultra–low material loss and flattened dispersion potentially has significant application in long distance transmission of terahertz signals. On the other hand, higher core power fraction properties potentially have wide application in terahertz wave guidance. Therefore, if the proposed fiber is utilized properly, it can open the door for convenient, efficient, long distance and flexible transmission of terahertz signals.

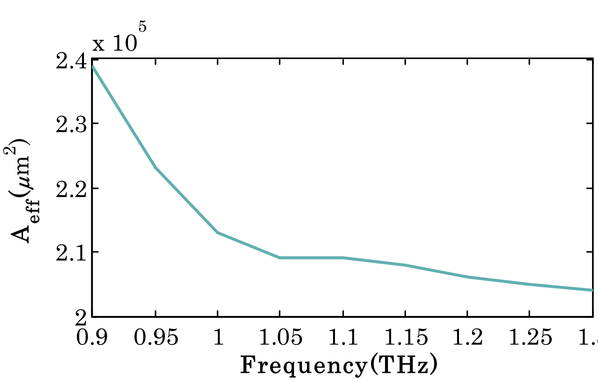

Fig. 11. Effective mode area as a function of frequency at D_{core} = 300 μm.

References

[1] R.H. Jacobsen, D.M. Mittleman, M.C. Nuss, Chemical recognition of gases and gas mixtures with terahertz waves, Opt. Lett. 21 (24) (1996) 2011–2013.
[2] M. Nagel, P.H. Bolivar, M. Brucherseifer, H. Kurz, A. Bosserhoff, R. Buttner, Integrated THz technology for label free genetic diagnostics, Appl. Phys. Lett. 80 (1) (2002) 154–156.
[3] W.L. Chan, J. Deibel, D.M. Mittleman, Imaging with terahertz radiation, Rep. Prog. Phys. 70 (8) (2007) 1325–1379.
[4] D.M. Mittleman, M. Gupta, R. Neelamani, R.G. Baraniuk, J.V. Rudd, M. Koch, Recent advances in terahertz imaging, Appl. Phys. B 68 (6) (1999) 1085–1094.
[5] H.T. Chen, R. Kersting, G.C. Cho, Terahertz imaging with nanometer resolution, Appl. Phys. Lett. 83 (15) (2003) 3009–3011.
[6] J.Q. Zhang, D. Grischkowsky, Waveguide terahertz time-domain spectroscopy of manometer water layers, Opt. Lett. 29 (14) (2004) 1617–1619.
[7] D. Pinto, S.S.A. Obayya, Improved complex envelope alternative direction implicit finite difference time domain method for photonic bandgap cavities, IEEE J. Lightwave Technol. 25 (2007) 440–447.
[8] S. Atakaramians, S. Afshar V, T.M. Monro, D. Abbott, Terahertz dielectric waveguides, Adv. Opt. Photonics 5 (2) (2013) 169–215.
[9] K. Wang, D.M. Mittleman, Metal wires for terahertz wave guiding, Nature 432 (7015) (2004) 376–379.
[10] B. Bowden, J.A. Harrington, O. Mitrofanov, Silver/polystyrene-coated hollow glass waveguides for the transmission of terahertz radiation, Opt. Lett. 32 (20) (2007) 2945–2947.
[11] A. Hassani, A. Dupuis, M. Skorobogatiy, Low loss porous terahertz fibers containing multiple sub-wavelength holes, Appl. Phys. Lett. 92 (2008) 071101.
[12] A. Hassani, A. Dupuis, M. Skorobogatiy, Porous polymer fibers for low-loss terahertz guiding, Opt. Express 16 (9) (2008) 6340–6351.
[13] L.J. Chen, H.W. Chen, T.F. Kao, J.Y. Lu, C.K. Sun, Low-loss sub-wavelength plastic fiber for terahertz waveguiding, Opt. Lett. 31 (3) (2006) 308–310.
[14] M. Nagel, A. Marchewka, H. Kurz, Low-index discontinuity terahertz waveguides, Opt. Express 14 (21) (2006) 9944–9954.
[15] C.S. Ponseca, R. Pobre, E. Estacio, N. Sarukura, A. Argyros, M.C.J. Large, M.A. van Eijkelenborg, Transmission of terahertz radiation using a micro-structured polymer optical fiber, Opt. Lett. 33 (9) (2008) 902–904.
[16] M. Goto, A. Quema, H. Takahashi, S. Ono, N. Sarukura, Teflon photonic crystal fiber as terahertz waveguide, Jpn. J. Appl. Phys. 43 (2B) (2004) L317–L319.
[17] K. Nielsen, H.K. Rasmussen, A.J.L. Adam, P.C.M. Planken, O. Bang, P. Uhd Jepsen, Bendable, low-loss TOPAS fibers for the terahertz frequency range, Opt. Express 17 (10) (2009) 8592–8601.
[18] X. Tang, Y. Jiang, B. Sun, J. Chen, X. Zhu, P. Zhou, D. Wu, Y. Shi, Elliptical hollow fiber with inner silver coating for linearly polarized terahertz transmission, IEEE Photonics Technol. Lett. 25 (2013) 331–334.
[19] H. Bao, K. Nielsen, O. Bang, P.U. Jepsen, Dielectric tube waveguides with absorptive cladding for broadband, low-dispersion and low loss THz guiding, Sci. Rep. 5 (2015) 7620.
[20] C. Markos, A. Stefani, K. Nielsen, H.K. Rasmussen, W. Yuan, O. Bang, High-Tg TOPAS microstructured polymer optical fiber for fiber Bragg grating strain sensing at 110 degrees, Opt. Express 21 (4) (2013) 4758–4765.
[21] G. Emiliyanov, J.B. Jensen, O. Bang, P.E. Hoiby, L.H. Pedersen, E.M. Kjær, L. Lindvold, Localized bio-sensing with TOPAS micro-structured polymer optical fiber, Opt. Lett. 32 (5) (2007) 460–462.
[22] W. Yuan, L. Khan, D.J. Webb, K. Kalli, H.K. Rasmussen, A. Stefani, O. Bang, Humidity insensitive TOPAS polymer fiber Bragg grating sensor, Opt. Express 19 (20) (2011) 19731–19739.
[23] J. Balakrishnan, B.M. Fischer, D. Abbott, Sensing the hygroscopicity of polymer and copolymer materials using terahertz time-domain spectroscopy, Appl. Opt. 48 (12) (2009) 2262–2266.
[24] G. Woyessa, A. Fasano, A. Stefani, C. Markos, K. Nielsen, H.K. Rasmussen, O. Bang, Single mode step-index polymer optical fiber for humidity insensitive high temperature fiber Bragg grating sensors, Opt. Express 24 (2) (2016) 1253–1260.
[25] G. Zhao, M.T. Mors, T. Wenckebach, P.C.M. Planken, Terahertz dielectric properties of polystyrene foam, J. Opt. Soc. Am. B 19 (6) (2002) 1476–1479.
[26] J.Y. Lu, C.P. Yu, H.C. Chang, H.W. Chen, Y.T. Li, C.L. Pan, C.K. Sun, Terahertz air-core microstructure fiber, Appl. Phys. Lett. 92 (6) (2008) 0641051–0641053.
[27] M. Skorobogatiy, A. Dupuis, Ferroelectric all-polymer hollow Bragg fibers for terahertz guidance, Appl. Phys. Lett. 90 (11) (2007) 1135141–1135143.
[28] S. Atakaramians, S. Afshar V, M. Nagel, H.K. Rasmussen, O. Bang, T.M. Monro, D. Abbott, Direct probing of evanescent field for characterization of porous THz fibers, Appl. Phys. Lett. 98 (2011) 121104.
[29] S.F. Kaijage, Z. Ouyang, X. Jim, Porous-core photonic crystal fiber for low loss terahertz wave guiding, IEEE Photonics Technol. Lett. 25 (15) (2013) 1454–1457.
[30] R. Islam, G.K.M. Hasanuzzaman, Md.S. Habib, S. Rana, M.A.G. Khan, Low-loss rotated porous core hexagonal single-mode fiber in THz regime, Opt. Fiber Technol. 24 (2015) 38–43.

[31] S. Rana, G. Kibria, Md. Hasanuzzaman, S. Habib, S.F. Kaijage, R. Islam, Proposal for a low loss porous core octagonal photonic crystal fiber for T-ray wave guiding, Opt. Eng. 53 (11) (2014) 115107.
[32] Md.I. Hasan, S.M. Abdur Razzak, G.K.M. Hasanuzzaman, Md.S. Habib, Ultra-low material loss and dispersion flattened fiber for THz transmission, IEEE Photonics Technol. Lett. 26 (23) (2014).
[33] R. Islam, S. Rana, Dispersion flattened, low-loss porous fiber for single-mode terahertz wave guidance, Opt. Eng. 54 (5) (2015) 055102.
[34] R. Islam, Md.S. Habib, G.K.M. Hasanuzzaman, S. Rana, A novel low loss diamond-core porous fiber for polarization maintaining terahertz transmission, IEEE Photonics Technol. Lett. 28 (14) (2016).
[35] Md.R. Hasan, Md.S. Anower, Md.I. Hasan, S.M.A. Razzak, Polarization maintaining low-loss slotted core kagome lattice thz fiber, IEEE Photonics. Technol. Lett. 28 (16) (2016).
[36] K. Nielsen, H.K. Rasmussen, P. Uhd Jepsen, O. Bang, Porous core honeycomb band gap THz fiber, Opt. Lett. 36 (2011) 666.
[37] S. Islam, M.R. Islam, M. Faisal, A.S.M.S. Arefin, H. Rahman, J. Sultana, S. Rana, Extremely low loss, dispersion-flattened porous core photonic crystal fiber for thz regime, Opt. Eng. 55 (7) (2016) 07611.
[38] N. Chen, J. Liangand, L. Ren, High-birefringence, low-loss porous fiber for single-mode terahertz-wave guidance, Appl. Opt. 52 (21) (2013) 5297–5302.
[39] H. Bao, K. Nielsen, H.K. Rasmussen, P.U. Jepsen, Fabrication and characterization of porous-core honeycomb bandgap THz fibers, Opt. Express 20 (28) (2012) 29507–29517.
[40] M.I. Hasan, M.S. Habib, M.S. Habib, S.M. Abdur Razzak, Design of hybrid photonic crystal fiber: polarization and dispersion properties, Photonics Nanostruct. Fundam. Appl. 12 (2) (2014) 205–211.
[41] R.T. Bisen, D.J. Trevor, Solgel-derived micro-structured fibers: fabrication and characterization, in: Proc. Optical Fiber Communication Conf., OFC, 2005.
[42] J.J. Bai, J.N. Li, H. Zhang, H. Fang, S.J. Chang, A porous terahertz fiber with randomly distributed air holes, Appl. Phys. B 103 (2) (2011) 381–386.
[43] K. Nielsen, H.K. Rasmussen, P. Uhd Jepsen, O. Bang, Broadband terahertz fiber directional coupler, Opt. Lett. 35 (2010) 2879.
[44] H. Bao, K. Nielsen, H.K. Rasmussen, P. Uhd Jepsen, O. Bang, Design and optimization of mechanically down-doped terahertz fiber directional couplers, Opt. Express 22 (8) (2014) 9486–9497.